JOURNAL OF VIROLOGY, Nov. 1986, p. 548–557
0022-538X/86/110548-10$02.00/0
Copyright © 1986, American Society for Microbiology
Vol. 60, No. 2

# Identification of the Major Structural and Nonstructural Proteins Encoded by Human Parvovirus B19 and Mapping of Their Genes by Procaryotic Expression of Isolated Genomic Fragments

SUSAN F. COTMORE,[1] VIRGIL C. McKIE,[2] LARRY J. ANDERSON,[3] CAROLINE R. ASTELL,[4] AND PETER TATTERSALL[1]*

*Departments of Laboratory Medicine and Human Genetics, Yale University School of Medicine, New Haven, Connecticut 06510[1]; Department of Pediatrics, School of Medicine, Medical College of Georgia, Augusta, Georgia 30912[2]; Division of Viral Diseases, Center for Infectious Diseases, Centers for Disease Control, Atlanta, Georgia 30333[3]; and Department of Biochemistry, Faculty of Medicine, University of British Columbia, Vancouver, British Columbia, Canada V6T 1W5[4]*

Received 21 April 1986/Accepted 31 July 1986

**Plasma from a child with homozygous sickle-cell disease, sampled during the early phase of an aplastic crisis, contained human parvovirus B19 virions. Plasma taken 10 days later (during the convalescent phase) contained both immunoglobulin M and immunoglobulin G antibodies directed against two viral polypeptides with apparent molecular weights of 83,000 and 58,000 which were present exclusively in the particulate fraction of the plasma taken during the acute phase. These two protein species comigrated at 110S on neutral sucrose velocity gradients with the B19 viral DNA and thus appear to constitute the viral capsid polypeptides. The B19 genome was molecularly cloned into a bacterial plasmid vector. Restriction endonuclease fragments of this cloned B19 genome were treated with BAL 31 and shotgun cloned into the open reading frame expression vector pJS413. Two expression constructs containing B19 sequences from different halves of the viral genome were obtained, which directed the synthesis, in bacteria, of segments of virally encoded protein. These polypeptide fragments were then purified and used to immunize rabbits. Antibodies against a protein sequence specified between nucleotides 2897 and 3749 recognized both the 83- and 58-kilodalton capsid polypeptides in aplastic plasma taken during the acute phase and detected similar proteins in the tissues of a stillborn fetus which had been infected transplacentally with B19. Antibodies against a protein sequence encoded in the other half of the B19 genome (nucleotides 1072 through 2044) did not react specifically with any protein in plasma taken during the acute phase but recognized three nonstructural polypeptides of 71, 63, and 52 kilodaltons present in the liver and, at lower levels, in some other tissues of the transplacentally infected fetus.**

The human parvovirus B19 was discovered in 1975 by Cossart et al. (7) in the plasma fraction of blood obtained from a small number of apparently asymptomatic blood donors. Although seroepidemiological studies showed that about 60% of adults in the United Kingdom had been infected with the virus (6) and that is a common cause of infection in children (13), widespread clinical interest in B19 was not aroused until 1981, when Pattison and colleagues demonstrated that it is responsible for aplastic crisis in children with homozygous sickle-cell disease (20, 25). It is now clear that this virus is the major etiologic agent of reticulocytopenic aplastic crisis in patients with a variety of hemolytic anemias (12, 14, 20, 21, 25) and that it is responsible for erythema infectiosum (fifth disease), a common, epidemic disease characterized by a lacy, measleslike rash seen predominantly in young children (3). Healthy adults infected with B19 usually show little overt disease, although many infected women may experience transient, and in some cases recurring, arthralgia following infection (2, 22, 36). Although the disease can be asymptomatic in adults, some infected pregnant women can transmit virus to their fetuses transplacentally (4). Prospective epidemiological studies are in progress to determine whether this virus is responsible for fetal demise or birth defects (E. Fridell, M. Grandien, and M. Anderson, EMBO Parvovirus Workshop Abstr. C/2, p. 17, 1985; see Materials and Methods), as has been shown to be the case for many of the parvoviruses which infect rodents and domestic animals.

We previously described (9) the characterization and molecular cloning of a B19 genome obtained from one of the original asymptomatic blood donors, B19-Wi, studied by Cossart. Together with a previous report by Summers et al. (28), this firmly established that B19 is a parvovirus, but DNA hybridization studies showed that it is only very distantly related to other serotypes in this family (9). In the present study, we describe the cloning of a second B19 genome (designated B19-Au), isolated from a plasma sample obtained from a child with homozygous sickle-cell disease, presenting in the early phase of an aplastic crisis at the Pediatric Sickle Cell Clinic of the Medical College of Georgia, Augusta, Ga. DNA-DNA hybridization studies (9) and restriction digest analysis showed that the B19-Wi and B19-Au genomes are very similar, although not identical, and we have recently confirmed and extended this observation by determining the DNA sequence of the entire B19-Au clone (26) and much of the sequence of the B19-Wi clone (M. C. Blundell and C. R. Astell, unpublished results). In this study, we used these two isolates in conjunction with diagnostic human anti-B19 sera to analyze the capsid proteins encoded by the virus. To identify the regions of the viral genome encoding these structural proteins as well as any viral nonstructural proteins, we shotgun cloned restriction fragments from the B19-Au genome into a procaryotic expression vector and isolated bacterial fusion proteins

* Corresponding author.

expressing sequences from both halves of the B19 genome. Antibodies raised against these proteins were used to identify the region of the genome containing the capsid genes and, by default, the region which did not encode capsid and which might therefore specify the nonstructural proteins. In this report, we describe the use of this approach to detect virus-specified proteins in serum taken during aplastic crisis in the acute phase and in tissue extracts derived from a stillborn fetus which had been infected transplacentally with B19.

## MATERIALS AND METHODS

**Materials.** Procaryotic expression vectors PJS413 and PHK414 7X were obtained, under license, from Molecular Genetics Inc., Minnetonka, Minn. Bacterial strains were the gift of Molecular Genetics Inc. and Lynn Enquist. Restriction endonucleases and other DNA-modifying enzymes were generally obtained from New England BioLabs, Inc., Beverly, Mass. Radioisotopes and reagents for DNA sequencing were obtained from Amersham Corp., Arlington Heights, Ill.

**Clinical case descriptions.** (i) Patient A, a 13 1/2-year-old male with documented homozygous sickle-cell anemia presented in aplastic crisis at the Pediatric Sickle Cell Clinic of the Medical College of Georgia on 1 December 1982. The initial hemogram revealed a hemoglobin level of 4.2 g/dl, a hemocrit of 11%, and a leukocyte count of 8,700 with 76% segmented neutrophils, 22% lymphocytes, and 2% monocytes. He had a reticulocyte count of 2.0% and an erythrocyte count of $1.3 \times 10^6$ with a mean cell volume of 84. The patient was immediately hospitalized, and serum and plasma samples were sent to Yale University for possible virus isolation. The patient was stabilized with hydration, oxygen, and partial-exchange transfusions, and over the next few days he rapidly recovered. Plasma was obtained, during the convalescent phase, on 10 December 1982, 10 days after initial presentation. (ii) Fetus B, a stillborn female, was identified in a prospective study of the outcome of pregnancy among women exposed to B19 during an epidemic of fifth disease. At 17 1/2 weeks of gestation, a routine ultrasound examination had suggested that this pregnancy was normal, but at 20 weeks the 18-year-old mother had presented with headache, fever, and nausea following a transient pruritic rash. At 24 weeks of gestation, the mother reported cessation of fetal movement. Following an ultrasound examination, labor was induced and a 420-g stillborn hydroptic fetus was delivered. Autopsy revealed fetal hydrops with generalized edema and autolysis of the viscera. Serum drawn from the mother at the time of delivery was positive for B19-specific immunoglobulin M (IgM) and IgG antibody by the enzyme-linked immunosorbent assay. Various tissue samples from this fetus were macerated in 50 mM Tris hydrochloride–5 mM EDTA (pH 8.7) with a Tekmar Stomacher homogenizer, and aliquots were analyzed for B19 DNA by slot-blot hydridation with an RNA probe synthesized from the riboprobe vector pYT104-V described below.

**Plasma fractionation and virus isolation.** Plasma samples (1.0 ml each) taken from patient A during the acute and convalescent phases of disease were centrifuged at 12,000 × *g* for 5 min, and the supernatant fraction was diluted to 2 ml with 100 mM Tris hydrochloride–1 mM EDTA (pH 8.7). This was then layered on 1.25 ml of 10% glycerol over 1.25 ml of 30% glycerol on top of a 0.25-ml 60% metrizamide cushion in an SW50.1 centrifuge tube (Beckman Instruments, Inc., Fullerton, Calif.). All solutions were made up in TE buffer (50 mM Tris hydrochloride, 0.5 mM EDTA [pH 8.7]). The step gradient was centrifuged at 48,000 rpm for 150 min at 5°C to separate soluble and particulate plasma components. These fractions were collected as the top 2.2 ml and the bottom 0.6 ml, respectively. The particulate fraction was then dialyzed exhaustively against TE buffer in the cold. Serum B19-Wi, a B19 antigen-positive serum originally identified by Cossart et al. (7), was also fractionated in this way. B19-Au viral DNA was found, by alkaline agarose gel electrophoresis, to be confined to the particulate fraction obtained from patient A and Wi plasma taken during the acute phase. Aliquots of the particulate fraction of patient A plasma taken during both the acute and convalescent phases were diluted to 100 μl in phosphate-buffered saline (pH 7.2) and iodinated for 5 min on ice by the Iodogen procedure (23) in the presence of 0.5 mCi of carrier-free $^{125}I$. After a further 5 min on ice in the absence of Iodogen, the labeled protein was separated from unincorporated $^{125}I$ by centrifugation through a microcolumn of Sephadex G-50 in phosphate-buffered saline containing 1 mg of bovine serum albumin per ml. Some of the $^{125}I$-labeled proteins from the patient A plasma particulate fraction were diluted with additional unlabeled particulate material from the same source and analyzed by velocity centrifugation on neutral sucrose gradients. Fractions were collected through the gradient and analyzed for protein by sodium dodecyl sulfate-polyacrylamide gel electrophoresis (SDS-PAGE) and for DNA by electrophoresis in alkaline agarose. Material from the particulate fraction obtained from patient A plasma taken during the acute phase was also disrupted with 0.3 N NaOH, and the DNA was isolated by centrifugation on alkaline sucrose gradients. Portions were collected throughout the gradients, and B19 DNA was detected by DNA hybridization. Positive fractions were pooled, dialyzed against 10 mM Tris hydrochloride, 1 mM EDTA (pH 7.0), and stored frozen at −20°C.

**Molecular cloning of the B19-Au viral genome.** The partially annealed viral DNA was melted by heating to 90°C for 2 min in TE buffer, and the palindromic sequences of the viral termini were used to prime the synthesis of complementary strands by using the Klenow fragment of *Escherichia coli* polymerase I, as previously described (9). *Eco*RI linkers were then ligated to the viral termini, and the DNA was cut with both *Eco*RI (which does not cut in the viral genome) and *Bam*HI, which cuts B19 DNA once at approximately map unit 76 (9). Each half of the genome was then cloned separately into pAT153 (31), which had been cut with *Eco*RI and *Bam*HI, by conventional techniques. Bacterial clones containing plasmids with the two appropriate viral inserts (B19 map units approximately 0 to 76 and 76 to 100) were identified, and the viral sequences were excised, ligated to each other, cut with *Eco*RI, and recloned as a full-length genome into the *Eco*RI site of pAT153. The viral insert in this clone, designated pYT103, has recently been sequenced (26) and shown to be an almost full-length copy of the viral genome. The only regions absent from the clone are a few hundred bases at the extreme 3′ and 5′ termini of the genome, but the entire coding sequence of the virus is present. This B19 insert was then excised with *Eco*RI, its ends were blunted with *E. coli* DNA polymerase I Klenow fragment, and it was ligated into the *Sma*I site of the "riboprobe" vector SP64 (Promega Biotech). Plasmids bearing both orientations of the B19 insert were isolated and designated pYT104-V and pYT104-C to indicate that RNA probes made from them detect strands equivalent in DNA sequence organization to the viral and complementary strands, respectively, of autonomous parvovirus which package only one strand sense (26).

**Procaryotic expression of protein sequences encoded by B19-Au.** The B19-Au genome contained in PYT103 was excised and digested with *Hin*fI to yield six fragments. This mixture was then digested briefly with BAL 31 nuclease, and the Klenow fragment of *E. coli* polymerase I was used, in the presence of all four deoxynucleotides, to blunt end all termini. The resulting mixture was ligated into a single *Sma*I site in the procaryotic expression vector pJS413 and introduced into *E. coli* NF1829. Foreign sequences $3n+1$ nucleotides long, which contain an open reading frame and which begin at nucleotide 1 of the first codon in this reading frame, can be expressed as the central part of a tripartite fusion protein when cloned into this site (27, 32–35). Such proteins are expressed under the control of the *lac* promotor-operator, and in *E. coli* strains such as NF1829 which express high levels of the *lac* repressor by virtue of the *laci*$^q$ gene located on the F factor, these proteins are not expressed unless specifically induced with lactose or isopropyl-β-D-thiogalactopyranoside (IPTG). The fusion proteins have β-galactosidase activity since their carboxy-terminal sequences are derived from a modified *lacZ* gene, and this activity is used to identify bacteria expressing foreign sequences. Full details of the expression vector, cloning strategy, and identification of appropriate clones have been reported elsewhere (10, 27, 32–34). The power of this expression system, as exemplified in the studies presented here, is that it provides a way of identifying regions of open reading frame and expressing proteins encoded by those sequences at high levels in bacteria without any prior knowledge of the DNA sequence or coding strategy of the virus.

Bacterial clones expressing two different B19 sequences were identified, and the plasmids carried by these bacteria were designated pYT105 and pYT106. After overnight induction with IPTG, such bacteria accumulate high levels of fusion proteins, which can be purified relatively easily. However, in this form they are usually insoluble and poorly immunogenic (10). To overcome these problems, an amber termination codon (TAG) was introduced immediately downstream of the B19 sequences, and the resulting plasmids (designated pYT105am and pYT106 am, respectively) were used to transform the bacterial strain LE392F, which is able to suppress partially such termination signals by virtue of suppressor tRNAs encoded by *supE* and *supF*. In this context, induction with IPTG leads to the synthesis and accumulation of both the full-length tripartite fusion protein and a truncated bipartite form which lacks the β-galactosidase sequences. This truncated form is easily purified from the full-length form by preparative SDS-PAGE and is both relatively soluble (depending on the nature of the viral sequences expressed) and highly immunogenic. To increase the levels of these proteins synthesized by induced bacteria, we then replaced the *lac* promoter in these constructs by the chimeric TAC promoter, as previously described (10).

**DNA sequencing.** Viral sequences expressed from pYT105 and pYT106 plasmids were identified by transferring a *Bgl*II-*Bam*HI fragment containing these sequences from the middle of the fusion gene into the *Bam*HI site of M13mp8, selecting clones in both orientations, isolating single-stranded DNA, and sequencing through the plasmid-virus junctions by using the universal primer and the dideoxynucleotide enzyme extension method of Sanger et al. (24).

**Antisera.** Reference diagnostic sera for the B19 capsid were P and Da (the gift of B. J. Cohen) and BD45642 (the gift of M. J. Anderson). Antisera against the genetically truncated amber fusion proteins synthesized from pYT105am and pYT106am were raised in male albino rabbits by the initial injection of about 200 μg of gel-purified protein in complete Freund adjuvant at multiple intramuscular and subcutaneous sites, followed by repeated injections of similar amounts of protein emulsified in incomplete Freund adjuvant at multiple subcutaneous sites during the next few months. Sera were collected 5 or 6 days after the last injection.

**In vitro translations.** mRNA from A9 cells infected with strain p of minute virus of mice, MVM(p), 324K cells infected with the autonomous parvoviruses LuIII or H-1, and EBTr cells infected with the autonomous bovine parvovirus (BPV) were prepared as previously described (8). RNA from HeLa cells coinfected with human adenovirus type 5 and adeno-associated virus type 2 (AAV-2) was kindly provided by Barrie Carter. The rabbit reticulocyte in vitro translation system has been described previously (8), and the analysis of the in vitro translation products of all of these viruses except AAV-2 has been published elsewhere (8, 10).

**Immunoprecipitation and Western blotting.** $^{125}$I-labeled samples from the particulate fraction derived from plasma taken from patient A during both the acute and convalescent phases of disease were immunoprecipitated essentially as described by Kessler (15) by using Formalin-fixed, heat-killed *Staphylococcus aureus* Cowan 1 cells. Samples were analyzed by SDS-PAGE as described by Laemmli (16), and gels were dried and autoradiographed by using XAR-5 film (Eastman Kodak Co., Rochester, N.Y.).

Both macerated samples and intact tissue fragments from fetus B were boiled in SDS sample buffer and analyzed by SDS-PAGE. Sample sizes were adjusted to be equivalent on the basis of Coomassie blue staining patterns. Proteins from duplicate gels were transferred to nitrocellulose by using a transblot chamber (Hoefer Scientific Instruments, San Francisco, Calif.), and the filters were incubated first with rabbit anti-B19 sera and then with goat anti-rabbit IgG conjugated with alkaline phosphatase (Bio-Rad Laboratories, Richmond, Calif.) essentially as described by Yen and Webster (37). Immunoreactive proteins were visualized by using the 5-bromo-4-chloro-3-indolyl phosphate/nitro blue tetrazolium color reactions as recommended by Bio-Rad. Molecular mass was determined by using prestained molecular weight markers (Diversified Biotech, Newton Center, Mass.) that were coelectrophoresed and co-transferred with the experimental samples.

## RESULTS

**Identification of the B19 capsid proteins in plasma taken during the acute aplastic phase.** Initial DNA hybridization analysis with a molecularly cloned B19-Wi genome (9) revealed that plasma taken from patient A during the acute phase contained 45 μg of B19 DNA per ml, while the plasma obtained 10 days later during the convalescent phase contained no detectable virus (less than 0.03 ng/ml). Thus the plasma taken during the acute phase but not that taken during the convalescent phase should contain the viral capsid proteins, while the plasma taken during the convalescent phase but not that taken during the acute phase might be expected to contain antibodies directed against the various proteins encoded by the viral agent responsible for the recent disease state. To explore this possibility, we fractionated plasma taken from patient A during the acute and convalescent phases by centrifugation through glycerol into supernatant and particulate components and labeled the

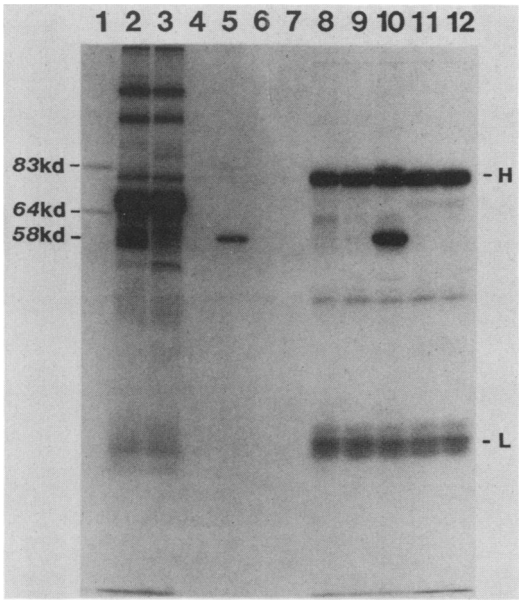


FIG. 1. Reciprocal immunoprecipitations with plasma taken during acute- and convalescent-phase aplastic crisis. Autoradiograph of an SDS-polyacrylamide gel (10%) of total proteins labeled with $^{125}I$ in the particulate fraction of plasma taken from patient A during the acute (lane 2) and convalescent (lane 3) phase before immunoprecipitation. These samples were immunoprecipitated as follows: particulate fraction from plasma taken during the acute phase precipitated with plasma taken during the acute phase (lane 4) or convalescent phase (lane 5); particulate fraction from plasma taken during the convalescent phase precipitated with plasma taken during the acute phase (lane 7) or convalescent phase (lane 6); particulate fraction from plasma taken during the acute phase precipitated with rabbit anti-human IgM alone (lane 8) or in conjunction with plasma taken during the acute phase (lane 9) or convalescent phase (lane 10); and particulate fraction from plasma taken during the convalescent phase precipitated with both rabbit anti-human IgM and plasma taken during the acute phase (lane 12) or convalescent phase (lane 11). Iodinated MVM(p) empty capsids are shown for size comparison (lane 1). Abbreviations: H, human (patient A) IgM heavy chain; L, human (patient A) IgM light chain.

proteins in aliquots of the pellet fractions with $^{125}I$. Gel electrophoresis in alkaline agarose showed that the pellet fraction from plasma taken during the acute phase contained all the B19 viral DNA detectable in the whole sample, as assessed by ethidium bromide staining (data not shown). A number of different protein species are present in the pellet fractions obtained from plasma during both acute and convalescent phases (Fig. 1, lanes 2 and 3). Although the compositions of the two pellets show a number of differences, it was not clear at this stage which, if any, of these were related to the presence of B19. However, when this labeled material was immunoprecipitated with antibodies present in the supernatant fraction of plasma taken during the convalescent phase (lane 5), two protein species with apparent molecular weights of 83,000 and 58,000 were identified. These two proteins were not present in the convalescent-phase sample (lane 6), and IgG antibodies directed against them were not present in plasma taken during the acute phase (lanes 4 and 7). This therefore suggested that the 83- and 58-kilodalton proteins were encoded by the infecting virus and, since they were in the pellet fraction, that they were probably the capsid proteins. Clearly, there is at least 10 times more $^{125}I$ associated with the 58-kDa species than than with the 83-kDa form, suggesting that the former may be the major protein species in the capsid; however, it remains possible that the relative differences in labeling intensity seen here merely reflect differences in the numbers of accessible tyrosine residues present in the two molecular species.

These immunoprecipitations depended upon the B19-specific antibody binding to *S. aureus* protein A and therefore detected predominantly complexes formed by using IgG antibodies. Since patient A had received a series of partial-exchange blood transfusions, IgG antibodies in his convalescent serum could theoretically have been derived passively from the transfused blood, but it is much less likely that IgM antibodies would be obtained by the same route, since only donors who had recently been infected with the virus would harbor such molecules (1). Similarly, if patient A had recently been infected with this virus for the first time, a strong IgM response might be expected. To analyze this possibility, we introduced rabbit anti-human IgM antibodies into the precipitation mixture. The anti-IgM antibodies precipitate IgM light and heavy chains from the labeled fractions even in the absence of specifically added first antisera (lane 8). However, when anti-IgM antibodies were added to plasma taken during the convalescent phase and the two were used together to precipitate particulate material from plasma taken during the acute phase, the 83- and 58-kDa proteins previously detected were precipitated in greatly increased amounts (lane 10), showing that convalescent serum from this patient contained both IgG and IgM antibodies directed against these two protein species.

If the 83- and 58-kDa proteins do constitute the B19-Au viral capsid, similar proteins should be present in the particulate fraction of B19-Wi serum. Plasma taken from patient A during the convalescent but not the acute phase precipitated these polypeptides (Fig. 2, lanes 9 and 10) in the same stochiometric proportions from B19-Wi serum as were precipitated from patient A plasma taken during the acute phase (lane 4). Moreover, various diagnostic human anti-B19 sera (Pi, Da, and BD45642) also recognize the 83- and 58-kDa species in B19-Wi and B19-Au plasma (lanes 5 through 8).

Finally, to establish that these two proteins were associated with the viral particle, we diluted the iodinated particulate fraction, taken from patient A during the acute phase in similar unlabeled material and analyzed this mixture by velocity sedimentation through a neutral sucrose gradient. The top fractions from this gradient contained most of the iodinated protein species, while most of the viral DNA cosedimented, in fractions 10 and 11, with the 83- and 58-kDa polypeptides in a peak coincident with 110S MVM full virions (Fig. 3). A second peak containing the 83- and 58-kDa proteins was also observed, centered around fraction 14. This peak cosedimented with 70S MVM empty capsids and contained large amounts of the putative viral capsid proteins but very little DNA. This suggests that it contains predominantly empty B19 capsids. It is not clear whether these particles are a natural product of B19 infection or are formed by disruption of full virions during purification. The presence of a small amount of viral DNA throughout this region of the gradient, presumably associated with partially disrupted virions, tends to suggest that the experimental conditions used do cause limited disruption of the B19 field isolate. Silver stain analysis of a similar gel also suggested that the 58-kDa protein constituted between 80 and 90% of the capsid proteins in both of these peaks (data not shown).

**Procaryotic expression of viral proteins.** Preliminary restriction endonuclease analysis of the B19-Wi and B19-Au

genomes cloned in plasmids pYT101, pYT102, and pYT103 had shown that although these two genomes were very similar, there were a number of differences which could be detected with, for example, the enzymes *Rsa*I, *Hha*I, and *Hin*fI. Despite this polymorphism, *Hin*fI appeared to be a useful enzyme for procaryotic expression studies, since it cut the B19-Au genome into six major fragments which varied in size between 500 and 1,000 base pairs. If, like the other parvoviruses for which sequence information was available at the time [MVM(p), H-1, and AAV-2], B19 had two major regions of open reading frame which together spanned almost the entire genome, such a digestion pattern should give at least two fragments of DNA containing continuous open reading frames. By analogy, one of these fragments would be derived from the 3′ half of the plus strand (by convention, the right-hand end) and would probably encode capsid sequences, while the other would originate from the left half of the genome and might therefore encode sequences expressed in nonstructural proteins. However, at the time these experiments were initiated, we did not know whether B19 had a plus and a minus strand or whether it used both strands to encode protein, and thus we were not able to select specific sequences for expression. Instead, the pJS413 procaryotic expression system we used permitted us to detect bacteria containing plasmids with any

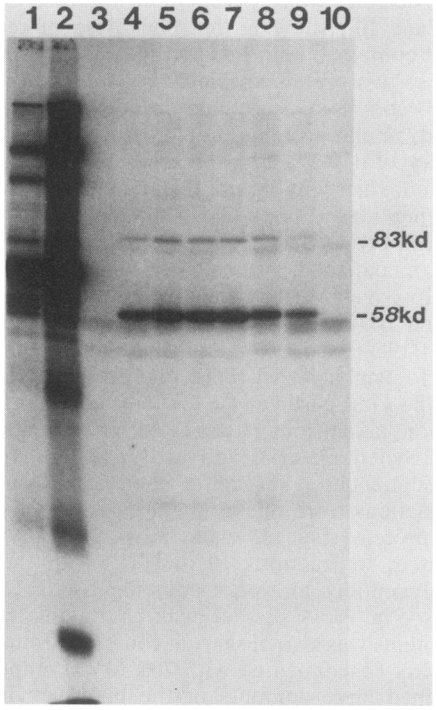


FIG. 2. Immunoprecipitation of iodinated proteins from acute phase plasma with B19 diagnostic antibodies. Autoradiograph of SDS-polyacrylamide gel (10%) showing total proteins labeled with $^{125}I$ in the particulate fraction of plasma taken from patient A during the acute phase (lane 1) or B19-Wi serum (lane 2) before immunoprecipitation. These samples were immunoprecipitated as follows: particulate fraction from patient A plasma taken during the acute phase precipitated with plasma taken from patient A during the acute phase (lane 3), plasma taken from patient A during the convalescent phase (lane 4), diagnostic antisera P (lane 5), BD45642 (lane 6), and Da (lane 7); B19-Wi particulate fraction precipitated with plasma taken from patient A during the acute phase (lane 10), plasma taken from patient A during the convalescent phase (lane 9), or the diagnostic P serum (lane 8).

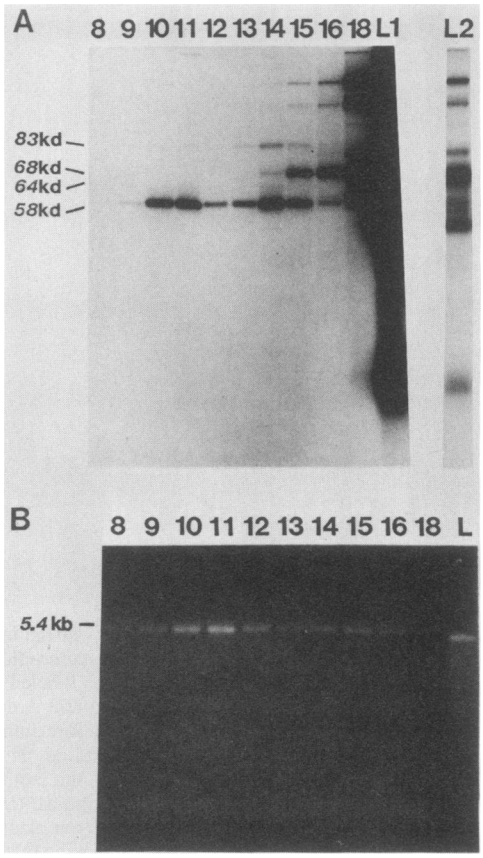


FIG. 3. Neutral glycerol gradient sedimentation of iodinated particulate fraction from plasma taken during the acute phase. (A) Autoradiograph of an SDS-polyacrylamide gel (10%) showing the total iodinated proteins loaded on to a neutral glycerol gradient (lane L1) and samples of material from various gradient fractions (designated 8 through 18 at the top of the figure). Lane L2 shows the total labeled proteins, as in lane L1, at a shorter exposure time. (B) Alkaline agarose gel (1%), stained with ethidium bromide, showing (lane L) B19-Au viral DNA (5.4 kilobase) in the material loaded onto the same neutral glycerol gradient as in panel A, and in samples taken from various gradient fractions. A similar sucrose gradient run in parallel with the one analyzed in this study was loaded with an extract of MVM(p)-infected A9 cells, and fractions were tested for their ability to hemagglutinate guinea pig erythrocytes. Peak agglutination was seen in fractions 11 (110S full particles) and 15 (70S empty capsids).

foreign open reading frame inserted in the correct orientation into a bipartite fusion gene. Thus we were able to shotgun clone a mixture of BAL-31-treated *Hin*fI fragments from B19 into the expression plasmid and use the bacteria to detect both the existence and the orientation of relatively large regions of open reading frame in the viral DNA. Using this approach, we repeatedly obtained clones expressing two sections of the viral genome. We recently determined the entire DNA sequence of the B19-Au genome resident in plasmid pYT103, which was used for these experiments (26). We use this sequence information to orient the *Hin*fI fragments of B19-Au with respect to the translation termination codons present in all three reading frames of the DNA strand thought to encode viral RNA (Fig. 4). Although the mRNA species transcribed by this virus have yet to be analyzed, only one of the DNA strands contains large stretches of open reading frame spanning most of the genome length, suggesting that this strand is probably responsible for encoding most, if not all, of the viral proteins. RNA polymerase II

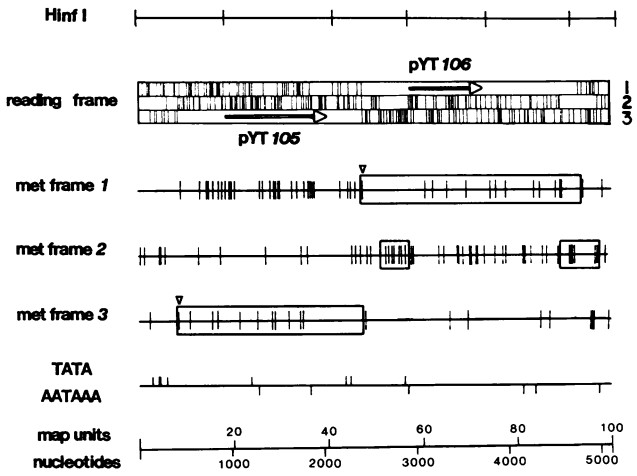


FIG. 4. Coding strategy of the B19-Au genome. The *Hin*fI sites in B19-Au and the genomic regions expressed in constructs pYT105 and pYT106 are shown in relation to a bar diagram depicting translation termination signals in all three reading frames of what is presumed to be the plus strand of the B19 genome. Lines labeled "met frames 1–3" use vertical bars to indicate the positions of methionine codons in the three reading frames, and boxed segments represent the major regions of open reading frame in this strand. Positions of TATA sequences and polyadenylation signals (AATAAA) are aligned for comparison with these blocks of coding sequence.

promoter consensus sequences and ATG codons in the presumed plus strand are also detailed in Fig. 4, together with the genome segments contained in the two typical expression plasmids pYT105 and pYT106, obtained from the viral genome cloned in pYT103. Construct pYT105 has a 973-base-pair insert and expresses 324 amino acids of viral protein encoded in this strand between nucleotides 1072 and 2044, while pYT106 has a 853-base-pair insert and expresses 284 amino acids of viral protein from this strand between nucleotides 2897 and 3749. The fragment cloned into pYT106 contains the B19-Au–B19-Wi *Hin*fI polymorphism; in B19-Wi, this region has an additional *Hin*fI site located approximately 40 bases from one end. A third expression clone containing sequences between nucleotides 3750 and 4636 should have been obtained if the B19-Au genome in pYT103 was exactly as described in Fig. 4. However, at position 3940 in pTY103 there is one adenine residue missing; this destroys the continuous open reading frame by switching it from one frame to another. This deletion was presumably introduced as the result of an error by the polymerase I Klenow fragment during the synthesis of the second strand prior to cloning (see Materials and Methods), since clones through this region of B19-Au prepared by annealing plus and minus viral strands do not show this frameshift mutation (26).

**Identification of the viral sequences encoding B19 capsid polypeptides.** When plasma taken from patient A during the acute and convalescent phases was subjected to Western blot analysis with rabbit antisera directed against the bipartite fusion protein expressed from pYT106am (containing B19-Au nucleotides 2897 to 3749), a major protein at 58 kDa and a somewhat less abundant protein at 83 kDa, which are only present in plasma taken during the acute phase, were identified (Fig. 5, lanes 1 through 3). These proteins, which have exactly the same apparent molecular masses as those previously described from the iodinated samples, are presumably the capsid polypeptides of B19. A faint but sharp band at about 64 kDa, which migrates below and is frequently distorted by the albumin band in plasma or serum samples (lanes 1 and 2), is also recognized by this antiserum in plasma taken during the acute phase and may form part of the viral capsid. A diffuse, broad band at around 50 kDa is detected in plasma taken during both acute and convalescent phases even in the absence of the rabbit anti-B19 serum. Since this band can be markedly diminished by preincubation of the plasma sample with protein A-Sepharose (lane 1), we assume that it is human immunoglobulin heavy chain which is being recognized by a minor population of antibodies present in the phosphatase-conjugated anti-rabbit IgG used in these studies, although this serum had been preabsorbed with human immunoglobulins by the supplier (Bio-Rad). Prolonged development of such blots also permits detection of a diffuse 25-kDa protein band in all serum samples; this is presumably the result of cross-reaction of anti-rabbit IgG antibodies with human immunoglobulin light chains.

In both pediatric and adult patients, B19 infection is known to involve serum viremia in which viral genomes and capsids are distributed throughout many tissues of the body. DNA-RNA hybridization studies revealed a similar widespread distribution of viral DNA in the tissues of fetus B, and Western blot analyses similarly detected the 83- and 58-kDa capsid proteins of B19 in all fetal tissues examined so far (thymus, heart, spleen, kidney, bone marrow, liver, and lung). Placenta samples, which may or may not have been fetal in origin, did not contain either viral DNA or these proteins. Figure 5, lanes 4 and 5, show the major 83- and

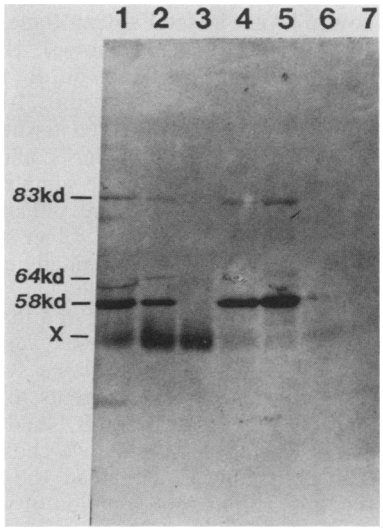


FIG. 5. Western blot analyses of B19 structural proteins. Antibodies directed against the fusion protein expressed from pYT106am were used to probe plasma taken from patient A during the acute and convalescent phases as well as tissue samples from B19-positive and -negative fetuses, separated by SDS-PAGE on a 10% gel, and transferred to nitrocellulose. This antiserum detects 83- and 58-kDa proteins in plasma taken from patient A during the acute phase (lanes 1 and 2) which are not detected in plasma taken during the convalescent phase (lane 3). The sample applied in lane 1 contained twice as much plasma as that loaded in lane 2 but had been preincubated with protein-A–Sepharose to remove much of the human immunoglobulin. As a consequence, the diffusely staining band marked X is substantially diminished in this sample. Lane 4 contains lung tissue, and lane 5 contains liver tissue from fetus B. Lanes 6 and 7 contain liver samples from aborted fetuses which were of similar age to fetus B and for which there was no evidence of B19 infection.

58-kDa proteins detected in fetal lung and liver samples. Although not particularly obvious in this figure, minor bands of around 64 and 70 kDa can also be detected in fetal liver samples if the phosphatase development reaction is prolonged. The 64-kDa molecule comigrates with a minor protein seen in plasma taken during the acute phase, whereas there is no counterpart of the 70-kDa molecule in plasma samples. Since these tissues may have been subjected to extensive autolysis prior to autopsy, we do not know whether these bands are naturally occurring precursor protein species involved in the formation of capsids in vivo or simply abnormal proteolytic products of protein VP-1 (see Discussion). Liver samples from two other spontaneously aborted fetuses which did not contain B19 DNA did not contain proteins which reacted with this antiserum (lanes 6 and 7).

**Identification of B19 nonstructural proteins in infected liver.** Antibodies directed against the fusion protein expressed by construct pYT105am (containing nucleotides 1072 through 2044 from B19-Au) do not recognize any proteins in plasma taken from patient A during the acute phase which are not also present in plasma taken during the convalescent phase (Fig. 6, lanes 5 and 6). However, the diffuse cross-reaction between human immunoglobulin heavy chains (50 kDa) and the phosphatase-labeled anti-rabbit IgG is still seen (X in Fig. 6), together with a faint, sharp, nonspecific band at 62 kDa. In contrast, liver tissue from the transplacentally infected fetus contains three major antibody-specific bands (lane 3). These bands, which have apparent molecular weights of around 71,000, 63,000, and 52,000 are also detected at a somewhat lower level in fetal lung tissue and at substantially lower levels in fetal spleen (lane 4), thymus, heart, and kidney tissue (data not shown). However, the relative proportions of the three bands do not appear to be exactly the same in all tissues. While the 71-kDa band is relatively easily detected in all infected tissues (including fetal bone marrow), the other two forms comigrate with a number of other proteins in most tissue samples and, when present at low concentrations, can be difficult to detect above nonspecific background staining. Liver samples from B19 DNA-negative fetuses do not contain any of these three antigenic species (lanes 1 and 2).

Since the studies reported above showed that antibodies against bacterially expressed B19 proteins were capable of efficiently detecting authentic B19 proteins synthesized in infected cells, we also used these reagents to explore the possible antigenic relatedness between B19 and a number of other parvoviruses. For these studies, we chose not to use Western blot analysis but used instead the much more sensitive approach of immunoprecipitation of viral proteins synthesized in vitro from viral mRNA, a technique not yet available to us for the study of B19 gene products because of the lack of a cell culture system with which to prepare infected cell RNA. Antisera against the fusion proteins synthesized from pYT105am and pYT106am completely failed to specifically immunoprecipitate proteins from the in vitro translation products of mRNA from cells infected with MVM(p), BPV, or AAV-2 (Fig. 7). Similar studies with mRNA from H-1- and LuIII-infected cells also proved negative. However the in vitro translations were normal and control precipitations with the appropriate antiviral antibodies were normal (Fig. 7). We take this to indicate that the regions of the B19 genome expressed in these constructs do not contain immunogenic stretches of linear polypeptide sequence which are conserved to any significant extent between different parvovirus serotypes. Whether these antibodies recognize native proteins encoded by the various viruses remains to be determined.

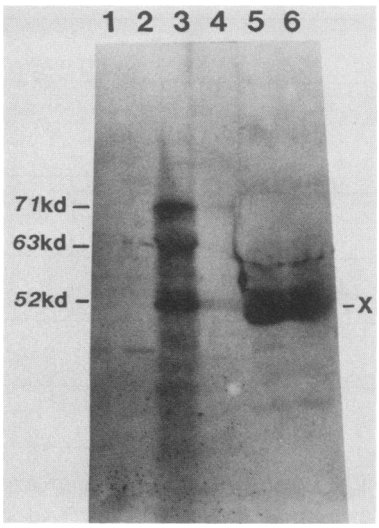


FIG. 6. Western blot analyses of B19 structural proteins. Antibodies directed against the fusion protein expressed from pYT105am were used to probe a protein blot similar to that shown in Fig. 5. This antiserum detects protein bands at 71, 63, and 52 kDa in liver tissue from fetus B (lane 3) which are not seen in the liver of uninfected fetuses (lanes 1 and 2). Spleen from fetus B also contains trace amounts of these proteins (lane 4). Plasma taken from patient A during the acute phase (lane 5) and convalescent phase (lane 6) do not contain these proteins, although a somewhat diffusely staining immunoglobulin heavy-chain band (X) and a faint band at 62 kDa are present.

## DISCUSSION

The data presented here demonstrate that the B19 virion present in plasma taken during acute-phase aplastic crisis contains two major proteins, with apparent molecular weights of 83,000 and 58,000, which we designate VP-1 and VP-2, respectively, for the purposes of this discussion. The results reported here do not agree with those of Clewley (5), who observed a major $^{125}$I-labeled protein of 48 kDa and two others of 68 and 80 kDa which comigrated with the viral DNA in a velocity sedimentation gradient. However, the consistency with which the several techniques we used detect both the 58- and 83-kDa polypeptides described here persuades us that these are the authentic structural polypeptides of the B19 virion. Precise measurements of the molar ratio of the two protein species were not possible, since all methods used to detect these proteins were indirect, but invariably there was at least 10 times more label or stain associated with the 58-kDa protein than with the 83-kDa molecule. In other parvoviruses, capsids are known to be assembled from a nested set of polypeptides in which the entire amino acid sequence of each of the smaller proteins is contained within the carboxy-terminal end of each successively larger polypeptide (19, 29). Our results suggest that B19 uses a similar strategy, since antibodies directed against the protein sequence encoded by a continuous stretch of open reading frame 853 nucleotides long recognize both of the capsid proteins. These capsid sequences are located in a major stretch of open reading frame in the right-hand half of the viral genome. In Fig. 4, the sequence cloned into the capsid expression construct pYT106am is indicated on a map of the B19-Au genome present in plasmid pYT103 (26). By

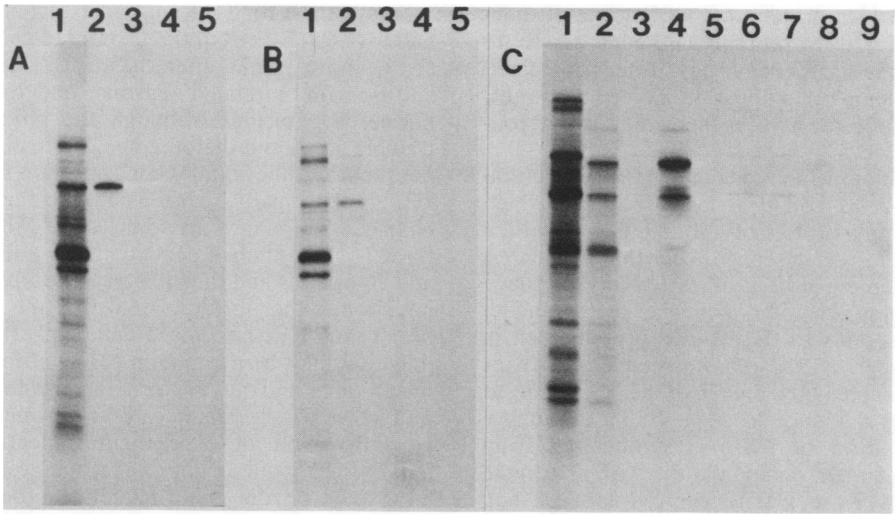


FIG. 7. Immunoprecipitation of parvoviral in vitro translation products with B19 specific antibodies. Autoradiographs of 10% polyacrylamide gels of the $^{35}S$-labeled in vitro translation products of mRNA extracted from cells infected with (A) MVM(p), (B) BPV, and (C) AAV-2. In panels A and B, lane 1 contains total translation products, lane 2 shows the capsid proteins immunoprecipitated with the appropriate rabbit anti-capsid antiserum, and lanes 3, 4, and 5 show that no proteins encoded by either MVM or BPV are precipitated by antisera against fusion proteins synthesized from pYT106am (lane 3), pYT105am (lane 4), or preimmune serum from the same rabbit as lane 4 (lane 5). In panel C, lane 1 contains the total translation products of mRNA from cells infected with adenovirus type 5 (lane 1), and coinfected with adenovirus type 5 and AAV-2 (lane 2). Lanes 3 and 4 are the same products as shown in lanes 1 and 2, respectively, immunoprecipitated with rabbit antiserum directed against AAV-2 capsids. Lanes 5 and 6 show the same pair of translation products as in lanes 2 and 1, respectively, immunoprecipitated with antiserum against the pYT106am fusion protein, and lanes 7 and 8 show the same products as in lanes 1 and 2, respectively, immunoprecipitated with antiserum against the pYT105am fusion protein. Lane 9 shows the same translation products as contained in lane 2 immunoprecipitated with preimmune serum from the rabbit used to generate the pYT105am protein-specific antibody.

analogy with the transcription strategy used by other parvoviruses, and given the arrangement of potential coding sequences and consensus RNA polymerase II promoter signals shown in Fig. 4, it seems likely that the transcript encoding the VP-1 polypeptide originates from a promoter in the middle of the genome, at map unit 45, and contains sequences specified throughout the entire length of the right-hand long open reading frame, perhaps initiating at the AUG codon at position 2444. Such an arrangement would give a protein of 781 amino acids with a real molecular weight of 99,900, which is somewhat greater than the apparent molecular weight seen here for VP-1, but still within the limits of experimental error for estimation by SDS-PAGE. A protein initiating at the next AUG codon downstream in this reading frame (at nucleotide 3125) would contain 554 amino acids and have a calculated molecular weight of 70,800. Again, this is larger than the apparent molecular weight estimated by SDS-PAGE for VP-2, i.e., 58,000. However, we believe that this allocation is likely to be correct, since in B19, the furthest downstream consensus promoter sequence is located at map unit 58, and if, as seems possible, this promoter is used to synthesize the mRNA specifying VP-2, ribosomes would have to read through, but ignore, the in-frame AUG at 3125 to start a VP-2 molecule with a lower actual molecular weight from any downstream AUG. The DNA fragment expressed in pYT106Am would therefore appear to specify 76 amino acids unique to the VP-1 molecule and the 208 residues of the VP-1–VP-2 common sequence located at the amino terminus of VP-2. The putative VP-1-specific regions of MVM and B19 share a region of relatively conserved amino acid sequence (50% perfect homology with MVM between B19 nucleotides 2815 to 2947 and 38% homology if the region is extended to B19 nucleotide 3058 [26]), suggesting that the overall structure of this part of the molecule is likely to be similar in the two viruses. However, although a large segment of this region is present in pYT106Am, we were unable to show antigenic cross-reactions between fusion protein and the in vitro translation products of capsid proteins from the autonomous parvoviruses MVM, LuIII, H-1, and BPV, suggesting that the conserved sequences are not immunogenic in this context. Similarly, we were unable to precipitate the in vitro-synthesized capsid proteins of AAV-2 with these antibodies, although the putative amino terminus of the VP-2 molecule of B19 shares regions of limited sequence homology with AAV-2 capsid polypeptides (26).

Antibodies against a fusion protein encoded by an expression construct (pYT105am) which contains B19 sequences derived from the left-hand open reading frame of the presumed plus strand (nucleotides 1072 through 2044) failed to recognize the B19 capsid polypeptides. However, liver from a transplacentally infected fetus contained three protein species with apparent molecular weights of 71,000, 63,000, and 52,000 which reacted specifically with the antibody. Thus this region of the genome must encode at least one nonstructural protein which is expressed in virally infected tissue. We do not know whether any of the three proteins seen in vivo correspond to the primary translation products of B19 mRNA. In the related virus MVM, the NS-1 gene encodes a protein with an apparent molecular weight of 83,000, which can be demonstrated by in vitro translation of virally encoded mRNA (8). Cells infected with MVM also contain a nuclear NS-1 protein of the same size, but higher-molecular-weight phosphorylated forms of NS-1 (10a) and smaller, processed forms of the molecule are also present (S. F. Cotmore and P. Tattersall, unpublished observations). Thus MVM-infected but otherwise relatively intact cells contain multiple processed forms of the single primary translation product of the NS-1 gene. For B19-infected cells in fetal liver there is the additional complication that the tissue was subject to autolysis prior to autopsy. However, even under these conditions, all the infected tissues con-

tained a detectable 71-kDa protein and all but one of them contained the 63- and 52-kDa proteins, although mostly in somewhat reduced amounts. Moreover, no tissues contained NS-1-specific bands of any other apparent molecular weight, suggesting that the three forms seen here may occur routinely in B19-infected cells.

The open reading frame which encodes the nonstructural polypeptides has an ATG codon at nucleotide 436 which could be used to initiate a protein of 671 amino acids with a molecular weight of 86,300. It seems likely that an mRNA encoding such a protein could be synthesized in vivo, since the necessary consensus promoter sequences are available, but whether it corresponds to the 71-kDa protein seen in these studies is not clear. B19 also has a second consensus promoter sequence located in the middle of the NS-1 gene, at map unit 24. There is evidence to suggest that an amino-terminally truncated form of NS-1 is synthesized from mRNAs initiating at a similar position in the AAV-2 genome (E. D. Sebring and J. A. Rose, EMBO Parvovirus Workshop Abstr. SII/2, p. 20, 1985). Transcripts arising from the second promoter in B19 would be expected to initiate protein synthesis at nucleotide 1288, giving rise to a 387-amino-acid molecule with a molecular weight of 49,300. Clearly this could correspond to the 52-kDa protein seen here, and it might be that such a promoter operates with variable efficiency in different cell types or at different stages in the viral infection.

There is a region of conserved amino acid sequence in the NS-1 genes of MVM, AAV-2, and B19 in which all three viruses show approximately 50% perfect amino acid homology over a region of about 135 residues. This sequence, between nucleotides 1390 and 1795 in B19, is present in the expression construct pYT105am, but antibodies against the fusion protein synthesized from this plasmid do not immunoprecipitate the nonstructural proteins of MVM, H-1, LuIII, BPV, or AAV-2 from in vivo translation products of viral mRNA. Since the nonstructural proteins of many of the autonomous parvoviruses show extensive antigenic cross-reactivity (8), the total lack of demonstrable cross-reaction between this relatively conserved region of the B19 nonstructural proteins and those of the other parvoviruses supports the contention that B19 is evolutionarily distant from any of the other known viruses. When full sequence information is available (for MVM, H-1, AAV-2, and B19), this disparity is very obvious (26), but even for other viruses such as BPV, DNA hybridization studies (9) and the antigenic analyses reported here totally fail to reveal a close relationship.

Clearly the most clinically significant observation reported here is the fact that liver, lung, and, to a much lesser extent, other tissues in a transplacentally infected fetus contained viral nonstructural gene products. Although under some rare and somewhat artificial situations in vitro this activity may not inevitably correlate with the production of infectious virus in the cell (11), in the correct host species in vivo it provides a fairly clear indication of whether and where viral replication is occurring. Thus the fetus examined here had received B19 from its mother and probably established a high-level viremia at least in part as a result of active viral replication in a number of its body tissues. There is, as yet, insufficient evidence to say whether transmission to the fetus is an inevitable consequence of infection during pregnancy, although it clearly did occur in the case we studied and has been reported previously (4). However, a recent retrospective seroepidemiologic study (17) reported that of eight women who developed rubelliform rashes and seroconverted for IgM antibodies against B19 during pregnancy (4 to 17 weeks), three suffered spontaneous abortions (1, 3, and 6 weeks after the rash), one had a therapeutic abortion for unrelated reasons, and three had apparently normal live births. Although the group studied was extremely small and the outcome of the eighth pregnancy was not reported, the spontaneous abortion rate observed (about 40%) is abnormally high and suggests that B19 infection does endanger pregnancy in some way. Moreover, two of the three live infants had persistent IgG antibodies to B19 at 12 and 16 months and thus had presumably experienced active infection, either in utero or within the first few months of life. Taken together, these data suggest that transplacental infection may be a common result of infection of the pregnant mother and may result in damage to the fetus depending on factors which remain to be determined. If a parallel can be drawn with the experimental infection of animals with parvoviruses, one might expect the gestational stage of the fetus to be a major factor influencing the outcome of such in utero infections (30). Typically, parvoviruses are limited to target cells which are both proliferating and of a particular set of differentiated phenotypes, aspects of their life cycle which explain to a great extent their classification as predominantly fetocidal and teratogenic agents. Thus, to understand the potential risks involved in transplacental infection with B19, we must establish which cell types in the developing fetus are susceptible to viral attack. The low levels of nonstructural protein observed, for example, in the spleen of the fetus examined in this study, could conceivably be due to blood-borne contamination from lytic replication occurring at other sites in the body. However, the relatively high levels of these proteins found in the liver and lung leaves little doubt that the virus is actively replicating in at least one cell type in these tissues. Since B19 causes a dramatic drop in the reticulocyte count in vivo (2) and is known to impair the development of certain erythroid progenitors in vitro (18), it is not particularly surprising that viral gene expression is active in fetal liver, since this tissue contains islands of haematopoeitic tissue. Similarly, replication in the lung tissue is not unexpected, since it is highly probable that B19 is transmitted as an infection of the respiratory tract (2) and that it therefore replicates in at least one cell type present therein. Immunohistochemical studies of infected fetal tissues may well provide the easiest approach to establishing exactly which cell type(s) is involved. Most adult tissues contain few cells undergoing mitosis and therefore afford little opportunity for parvoviral invasion and replication unless the virus strain is able to infect a cell type which is constantly proliferating in the course of tissue maintenance. In the fetus, however, many more cell types are undergoing cell division, and it may be that B19, although predominantly hematotropic in the adult, will be seen to have a more extensive tissue tropism repertoire when fetal tissues are examined in detail.

## ACKNOWLEDGMENTS

We thank Bernard Cohen for B19-Wi antigen containing serum and for the anti-B19 diagnostic sera P and Da. Serum BD45642 was the kind gift of Mary Anderson. We are indebted to Edith and Mary Beth Gardiner, who were instrumental in suggesting and organizing the transfer of samples between Augusta and New Haven and to Titus Huisman for his support of this collaboration. We thank Charles H. Woernle, Mississippi State Department of Health, Jackson, Miss., who reported the case of Fetus B to the Centers for Disease Control and collected the necessary sera and tissue samples. We are grateful to Molecular Genetics Inc. and to Lynn Enquist, Roger Watson, and John Salstrom for their advice and help

with the expression vector system. Barrie Carter kindly supplied RNA from AAV2- and adenovirus type 5-coinfected cells and rabbit antiserum directed against the AAV capsid, and Robert Bates generously provided rabbit antiserum (no. 0118) directed against the BPV capsid.

This work was supported by Public Health Service grants CA 29303 and AI 21118 from the National Cancer Institute and the National Institute for Allergy and Infectious Diseases, respectively.

## LITERATURE CITED

1. **Anderson, M. J., L. R. Davis, S. E. Jones, and J. R. Pattison.** 1982. The development and use of an antibody capture radioimmunoassay for specific IgM to a human parvovirus-like agent. J. Hyg. **88**:309–324.
2. **Anderson, M. J., P. G. Higgins, L. R. Davis, J. S. Willman, S. E. Jones, I. M. Kidd, J. R. Pattison, and D. A. J. Tyrrell.** 1985. Experimental parvoviral infection in humans. J. Infect. Dis. **152**:257–265.
3. **Anderson, M. J., E. Lewis, I. M. Kidd, S. M. Hall, and B. J. Cohen.** 1984. An outbreak of erythema infectiosum associated with human parvovirus infection. J. Hyg. **93**:85–93.
4. **Brown, T., A. Anand, L. D. Ritchie, J. P. Clewley, and T. M. S. Reid.** 1984. Intrauterine parvovirus associated with hydrops fetalis. Lancet **ii**:1033–1034.
5. **Clewley, J. P.** 1984. Biochemical characterization of a human parvovirus. J. Gen. Virol. **65**:241–245.
6. **Cohen, B. J., P. P. Mortimer, and M. S. Periera.** 1983. Diagnostic assays with monoclonal antibodies for the human serum parvovirus-like virus (SPLV). J. Hyg. **91**:113–130.
7. **Cossart, Y. E., B. Cant, A. M. Field, and D. Widdows.** 1975. Parvovirus-like particles in human serum. Lancet **i**:72–73.
8. **Cotmore, S. F., L. J. Sturzenbecker, and P. Tattersall.** 1983. The autonomous parvovirus MVM encodes two nonstructural proteins in addition to its capsid polypeptides. Virology **129**:333–343.
9. **Cotmore, S. F., and P. Tattersall.** 1984. Characterization and molecular cloning of a human parvovirus genome. Science **226**:1161–1165.
10. **Cotmore, S. F., and P. Tattersall.** 1986. Organization of the nonstructural genes of the autonomous parvovirus minute virus of mice. J. Virol. **58**:724–732.

10a. **Cotmore, S. F., and P. Tattersall.** 1986. The NS-1 polypeptide of the autonomous parvovirus MVM is a nuclear phosphoprotein. Virus Res. **4**:243–250.

11. **de Foresta, F., J. Deleys-Hertoghs, J. Cornelis, B. Klein, and J. Rommelaere.** 1985. Transformation by SV40 virus sensitizes fibroblasts of human skin to the lytic action of H-1 parvovirus. C.R. Seances Soc. Biol. Fil. **179**:276–282.
12. **Duncan, J. R., C. G. Potter, M. D. Capellini, J. B. Kurtz, M. J. Anderson, and D. J. Weatherall.** 1983. Aplastic crisis due to parvovirus infection in pyruvate kinase deficiency. Lancet **ii**:14–16.
13. **Edwards, J. M. B., I. Kessel, S. D. Gardner, B. R. Eaton, F. M. Pollock, D. G. Fleck, P. Gibson, M. Woodruff, and A. D. Porter.** 1981. The search for a characteristic illness in children with serological evidence of viral or toxoplasma infection. J. Infect. **3**:316–323.
14. **Kelleher, J. F., N. L. C. Luban, P. P. Mortimer, and T. Kamimura.** 1983. Human serum "parvovirus": a specific cause of aplastic crisis in children with hereditary spherocytosis. J. Pediatr. **102**:720–722.
15. **Kessler, S. W.** 1975. Rapid isolation of antigens from cells with a staphylococcal protein A-antibody adsorbent: parameters of the interaction of antibody-antigen complexes with protein A. J. Immunol. **115**:1617–1624.
16. **Laemmli, U. K.** 1970. Cleavage of structural proteins during the assembly of the head of bacteriophage T4. Nature (London) **227**:680–685.
17. **Mortimer, P. P., B. J. Cohen, M. M. Buckley, J. E. Cradock-Watson, M. K. S. Ridehalgh, F. Burkhardt, and V. Schilt.** 1985. Human parvovirus and the fetus. Lancet **ii**:1012.
18. **Mortimer, P. P., R. K. Humphries, J. G. Moore, R. H. Purcell, and N. S. Young.** 1983. A human parvovirus-like virus inhibits haematopoietic colony formation in vitro. Nature (London) **302**:426–429.
19. **Paradiso, P. R., K. R. Williams, and R. L. Constantino.** 1984. Mapping of the amino terminus of the H-1 parvovirus major capsid protein. J. Virol. **52**:77–81.
20. **Pattison, J. R., S. E. Jones, J. Hodgson, L. R. Davis, J. M. White, C. E. Stroud, and L. Murtaza.** 1981. Parvovirus infections and hypoplastic crisis in sickle cell anaemia. Lancet **i**:664–665.
21. **Rao, K. R. P., A. R. Patel, M. J. Anderson, J. Hodgson, S. E. Jones, and J. R. Pattison.** 1983. Infection with parvovirus-like virus and aplastic crisis in chronic haemolytic anaemia. Ann. Intern. Med. **98**:930–932.
22. **Reid, D. M., T. Brown, T. M. S. Reid, J. A. N. Rennie, and C. J. Eastmond.** 1985. Human parvovirus associated arthritis, a clinical and laboratory description. Lancet **i**:422–425.
23. **Salacinski, P. R. P., C. McLean, J. E. C. Sykes, V. V. Clement-Jones, and P. J. Lowry.** 1981. Iodination of proteins, glycoproteins, and peptides using a solid-phase oxidizing agent, 1,3,4,6-tetrachloro-3a,6a-diphenyl glycoluril (Iodogen). Anal. Biochem. **117**:136–146.
24. **Sanger, F., S. Nicklen, and A. R. Coulson.** 1977. DNA sequencing with chain terminating inhibitors. Proc. Natl. Acad. Sci. USA **74**:5463–5467.
25. **Serjeant, G. R., K. Mason, J. M. Toplay, B. E. Serjeant, J. R. Pattison, S. E. Jones, and R. Mohamed.** 1981. Outbreak of aplastic crisis in sickle cell anaemia associated with parvovirus-like agent. Lancet **ii**:595–597.
26. **Shade, R. O., M. C. Blundell, S. F. Cotmore, P. Tattersall, and C. R. Astell.** 1986. Nucleotide sequence and genome organization of human parvovirus B19 isolated from the serum of a child during an aplastic crisis. J. Virol. **58**:921–936.
27. **Silhavy, T. J., M. L. Berman, and L. W. Enquist.** 1984. Experiments with gene fusions. Cold Spring Harbor Laboratory, Cold Spring Harbor, N.Y.
28. **Summers, J., S. E. Jones, and M. J. Anderson.** 1983. Characterization of the genome of the agent of erythrocyte aplasia permits its classification as a human parvovirus. J. Gen. Virol. **64**:2527–2532.
29. **Tattersall, P., A. J. Shatkin, and D. C. Ward.** 1977. Sequence homology between the structural polypeptides of minute virus of mice. J. Mol. Biol. **111**:375–394.
30. **Toolan, H. W.** 1978. Maternal role in susceptibility of embryonic and newborn hamsters to H-1 parvovirus, p. 161–176. *In* D. C. Ward and P. Tattersall (ed.), Replication of mammalian parvoviruses. Cold Spring Harbor Laboratory, Cold Spring Harbor, N.Y.
31. **Twigg, A. J., and D. Sherrat.** 1980. Transcomplementable copy-number mutants of plasmid Col E1. Nature (London) **283**:216–218.
32. **Watson, R. J., J. H. Weis, J. S. Salstrom, and L. W. Enquist.** 1982. Herpes simplex virus type 1 glycoprotein D gene: nucleotide sequence and expression in Escherichia coli. Science **218**:381–384.
33. **Watson, R. J., J. H. Weis, J. S. Salstrom, and L. W. Enquist.** 1984. Bacterial synthesis of herpes simplex type 1 and 2 glycoprotein D antigens. J. Invest. Dermatol. **83**:102–111.
34. **Watson, R. J., J. H. Weis, J. S. Salstrom, and L. W. Enquist.** 1985. Expression of herpes simplex virus type 1 and type 2 glycoprotein D genes using the *Escherichia coli* lac promoter, p. 327–352. *In* Y. Becker (ed.), Recombinant DNA research and viruses. Martinus Nijhoff, The Hague, The Netherlands.
35. **Weis, J. H., L. W. Enquist, J. S. Salstrom, and R. J. Watson.** 1983. An immunologically active chimeric protein containing herpes simplex type 1 glycoprotein D. Nature (London) **302**: 72–74.
36. **White, D. G., A. D. Woolf, P. P. Mortimer, B. J. Cohen, D. R. Blake, and P. A. Bacon.** 1985. Human parvovirus arthropathy. Lancet **i**:419–422.
37. **Yen, T. S. B., and R. E. Webster.** 1981. Bacteriophage f1 gene II and X proteins. J. Biol. Chem. **256**:11259–11265.